Presented at the IXth International
Conference on High Energy Accelerators,
SLAC, Stanford, Ca., May 2-7, 1974.

LBL-2488
c.2

OBSERVATIONS ON COLLECTIVE LONGITUDINAL INSTABILITIES IN ELECTRON RINGS

A. Faltens, G. R. Lambertson,
J. M. Peterson and J. B. Rechen

May 1974

JUL 30 1974

Prepared for the U. S. Atomic Energy Commission
under Contract W-7405-ENG-48

TWO-WEEK LOAN COPY

This is a Library Circulating Copy which may be borrowed for two weeks. For a personal retention copy, call Tech. Info. Division, Ext. 5545

LAWRENCE BERKELEY LABORATORY
UNIVERSITY OF CALIFORNIA
BERKELEY

LBL-2488
c.2

DISCLAIMER

This document was prepared as an account of work sponsored by the United States Government. While this document is believed to contain correct information, neither the United States Government nor any agency thereof, nor the Regents of the University of California, nor any of their employees, makes any warranty, express or implied, or assumes any legal responsibility for the accuracy, completeness, or usefulness of any information, apparatus, product, or process disclosed, or represents that its use would not infringe privately owned rights. Reference herein to any specific commercial product, process, or service by its trade name, trademark, manufacturer, or otherwise, does not necessarily constitute or imply its endorsement, recommendation, or favoring by the United States Government or any agency thereof, or the Regents of the University of California. The views and opinions of authors expressed herein do not necessarily state or reflect those of the United States Government or any agency thereof or the Regents of the University of California.

Observations on Collective Longitudinal Instabilities in Electron Rings

A. Faltens, G.R. Lambertson, J.M. Peterson, J.B. Rechen

Lawrence Berkeley Laboratory
University of California
Berkeley, California

The longitudinal collective instability, or negative-mass effect, has been observed in a wide variety of particle beams. It has been a particularly bothersome effect in electron-ring systems. In order to understand its complicated, non-linear behavior and to find means of controlling this instability, we have made a series of radio-frequency and momentum-spread observations.

The theory of the negative-mass effect predicts a threshold intensity for the onset of growth of the instability -- namely, that the number of electrons N_e at which the electromagnetic bunching forces predominate over the dispersing action produced by an energy spread ΔE is given by[1]

$$N_e = |\eta| \frac{\gamma R Z_o}{2\beta^3 r_e |Z_n|/n} \left(\frac{\Delta E}{E}\right)^2$$

where η is the chromaticity (relative change in revolution frequency per unit momentum change), γ is the total energy in units of the rest mass, R is the major radius of the electron ring, Z_o is 377 ohms, β is the electron velocity in units of velocity of light, r_e is the classical electron radius, $\Delta E/E$ is the fractional energy spread (FWHM), and Z_n is the longitudinal coupling impedance seen by the electron ring for azimuthal modulation at the nth harmonic of the electron revolution frequency. Z_n is defined by the relationship $I_n Z_n = 2\pi R \mathcal{E}_n$, where $\mathcal{E}_n$ is the nth harmonic electric field strength at the ring, and I_n is the amplitude of the nth harmonic of the ring current. The key parameters at our disposal were the energy spread of the electron beam and the longitudinal coupling impedance.

The instantaneous energy spread of the electron beam from the 3.6 MeV injector was found to be less than 0.2% (FWHM). Spreads of 1, 2, or 4% were produced by passing the beam through non-uniform energy absorbers with sawtooth thickness profiles.

The longitudinal coupling impedance was controlled by means of conducting side plates, or "liners", placed inside the vacuum chamber rather close to the electron ring. The geometry of that inner section of our electron-ring compressor is illustrated in Figure 1.

The coupling impedance of an electron ring in this system is compared in Figure 2 with the impedance for a ring in free space and also with that of a ring between infinite sideplates. The use of close sidewalls of infinite extent would lower the impedance at all frequencies for which the axial spacing is less than or comparable to a half wavelength. With sidewalls separated by 5 cm, this critical frequency is about the 10th harmonic of the revolution frequency of an electron ring of 17 cm radius. At higher frequencies waves can propagate in this semi-infinite system, and the impedance approaches the free-space impedance. Our sideplates were not infinite in extent but rather were terminated by a conducting wall at a radius of about 22 cm and thus formed a resonant cavity having TE modes at frequencies higher than the 10th harmonic. The lowest mode resonant with an electron ring at 17 cm occurs at the 16th harmonic of the revolution frequency. The impedance in this resonance region is qualitatively indicated in Fig. 2 as very structured and having a typical value some Q times the impedance of the infinite side-plate case. We reduced the Q by the use of resistive material and holes. The inflector window and its attached cable assembly complicated the impedance picture throughout the frequency spectrum; its resonances were reduced in some assemblies by shunting the inflector window with resistive material. The conducting walls were usually stainless steel of about 12 micron thickness, which had effectively high conductance at radio frequencies and yet did not distort significantly the pulsed compressor field.

In our experiments we varied the following parameters: incident beam intensity (without change of emittance), pulse length (1/2-turn and 2-turn incident beam lengths), instantaneous energy spread (0.2 to 4% FWHM), energy ramp (up to 2% per turn), beam-to-sidewall spacing (± 1.5, ± 2.0, and ± 2.5 cm), and frequency of observation (all harmonics up to n = 40, usually in broad bands).

Radiofrequency activity was often seen to occur very soon after the formation of the electron ring. At the highest beam intensities the instability could be seen to develop even during the injection process, where it was strong enough to have a noticeable effect on the inflection process. Either lower intensity or greater injected energy spread resulted in later onset, slower growth rate, and smaller peak amplitude of the r.f. signal. The latest onset observed before the signal became undetectably low was as late as 1 microsecond. Typical envelopes of the radio-frequency signals are shown in Figure 3. One striking feature of these patterns of radio frequency amplitudes is that they appear to be independent of frequency over a broad range of observation -- i.e., for a given ring intensity and amount of energy spread, the R.F. envelope at the 12th harmonic, for example, had very closely the same shape and timing as that at the 20th or the 40th harmonic, which indicates strong coupling between the longitudinal bunching modes.

The variation of the peak r.f. activity with frequency qualitatively followed the impedance curve of Fig. 2. Typical data for a ring of 1.1×10^{12} electrons are shown in Fig. 4 for side-walls at ± 2.5 cm. With this sidewall spacing growth in the first few harmonics was not seen, which is consistent with the low coupling impedance expected at these frequencies. When the spacing to the sidewall was reduced to ± 1.5 cm, the peak activities at the high harmonics decreased, as expected, but here strong activity in the 2nd and 3rd harmonics did appear. The growth of low harmonic activity is seen also at a sidewall spacing of ± 2.0 cm, but in this case it was less severe and was reduced by shunting the inflector window with resistive material. Apparently at the closer spacings to the beam, the ring couples more strongly to the inflector window and finds a substantial coupling impedance due to resonances in the inflector system. Although the low harmonic behavior is worse in the ± 2.0 cm sidewall system, the high harmonic activity is, as expected, better (approximately by a factor of 5) than in the ± 2.5 cm case.

The radiofrequency voltage from the pick-up loops is interpreted as a measure of azimuthal modulation of

of the electron density. The maximum relative modulation is shown in Fig. 5 as the ratio of the maximum r.f. signal to the electron current. These data as well as measurements at other frequency bands display no threshold behavior; the modulation appears to be proportional to a power of the current. However, it is notable that the current that produces a given modulation increases in proportion to ΔE^2 in apparent but unexplained similarity to the threshold formula. The rule appears not to apply in the case of 0.2% ΔE because with this small energy spread, the spread of azimuthal frequencies is predominantly contributed by betatron amplitude spread. At injection, the betatron oscillations are quite non-linear and hence the effective equivalent energy spread for this case is at least 1/2%. This effective spread has been confirmed from observations of the damping rate of stable, low-frequency modulation at low intensity.

In a further effort to determine the threshold for the instability we measured the growth rate by observing the doubling time τ_2 (see Fig. 3). One expects[2] the growth rate $1/\tau_2$ to be zero at threshold current, I_{th}, and to approach zero as a smooth function of I that depends on the distribution of energies in the beam. In Figs. 6 and 7 values of $1/\tau_2$ are shown. One sees that larger growth rates arise for lower energy spread, as expected, but threshold currents indicated by extrapolating to zero do not exhibit the variation with energy spread that is expected from instability theory.

An alternate attempt to find a sensible threshold behavior was tried using the time τ_1 from injection to a standard low level of modulation [defined by V_{RF}(volts) = .025 I_{RING}(amps)]. An example of these data plotted again as growth rate, $1/\tau_1$, is shown in Fig. 8. Again, for zero growth rate, the data converge toward indicated thresholds near 2 or 3 amperes and show little dependence on energy spread.

The question next arises as to the significance of these longitudinal instabilities with respect to electron ring properties. What momentum spread is produced, and what damage is done to the beam? One damage caused by the negative-mass effect is the limitation in intensity that can be achieved. With high impedance sidewalls we were limited typically to about 1×10^{12} electrons trapped, whereas with the conducting sidewalls at $\pm$ 2.5 cm, we have had at least 5 times as much. The amount of energy spread was measured by the two-probe method;[3] the results are shown in Figure 9. We see that with very little incident energy spread the instability at high ring intensities can produce energy spread in excess of 5%. At this level it is beginning to be unacceptable because it increases the ring radial width to such an extent that the holding power is seriously reduced. With injected energy spreads of 1 and 2%, the instabilities are not strong enough to increase the energy spread further, even at ring intensities considerably higher than the calculated thresholds assuming $|Z_n|/n$ of 100 ohms.

The conclusions that we can draw from these studies are as follows:

1) A conducting enclosure can be designed to suppress longitudinal instability in the electron ring. Resonant responses of the enclosure appear but can be limited in strength.

2) The longitudinal instability is still a limiting but not necessarily prohibitive factor in achieving high electron density during the ring formation and start of compression. Throughout subsequent stages of the ring manipulation it is expected to require control.

3) The instability arises at many frequencies simultaneously and appears to be a non-linear phenomenon involving many coupled modes.

4) One does not observe a threshold for bunching that follows the usual linear predictions for a smooth energy distribution. Growing modulation is seen over a wide range of conditions.

5) Even in the presence of r.f. activity, deterioration of ring quality is moderate until intensities exceed the expected threshold to a significant degree. There is reason to believe that the commonly-accepted intensity limitations can be achieved or exceeded.

References

1. K. Hübner, E. Keil, and B. Zotter, Proc. VIII International Conf. on High Energy Accelerators, 295-297 (CERN, Geneva, Switzerland; 1971).

2. D. Möhl, LBL Internal Report ERAN-178, 1971 (unpublished).
P. Channell, LBL Internal Reprot ERAN-240, 1974 (unpublished).

3. J.M. Peterson and J.B. Rechen, 1973 Particle Accelerator Conference, IEEE Trans. on Nucl. Sci. NS-20, #3, p. 790 (1973).

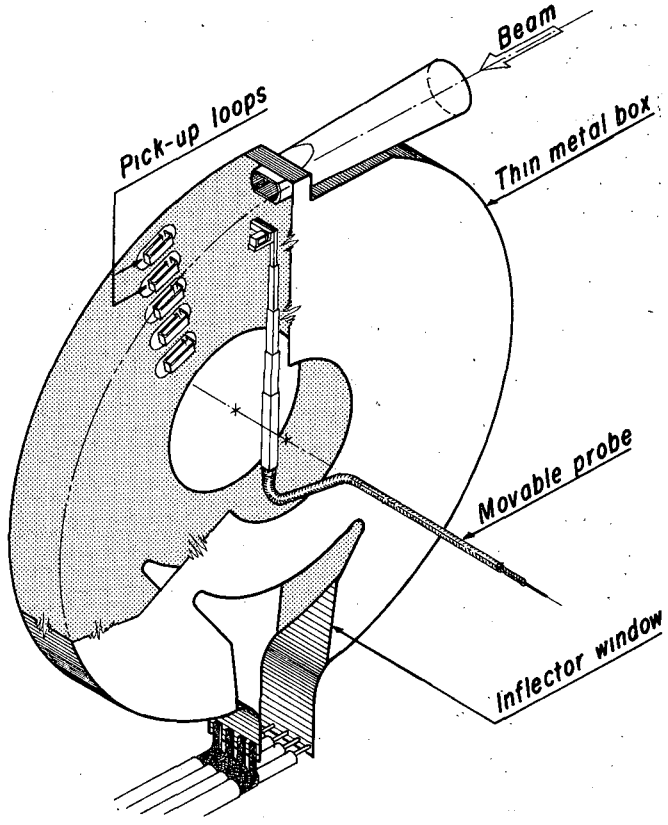

INNER WALLS OF COMPRESSOR

Figure 1 - Drawing of a typical conducting enclosure used in Compressor 4. The walls are 12 micron stainless steel. The pickup loops monitored beam level and radio-frequency activity. The movable probe functioned as a movable obstacle, a current collector, and a magnetic pickup loop.

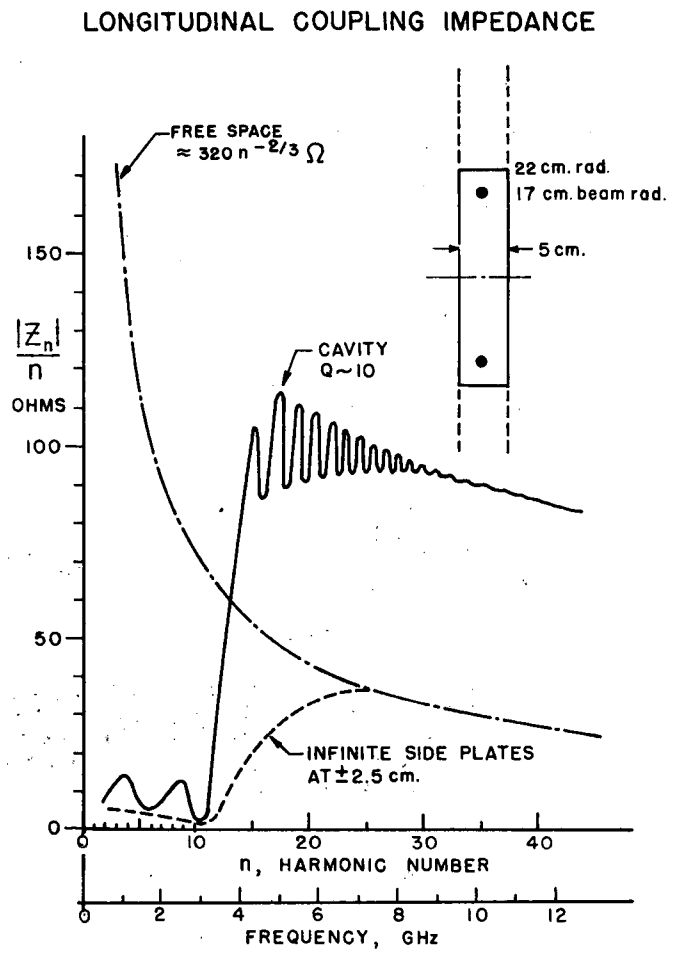

Figure 2 - Approximate variation of the longitudinal coupling impedance of an electron ring (a) in free space, (b) between infinite sideplates, and (c) in an enclosed cavity.

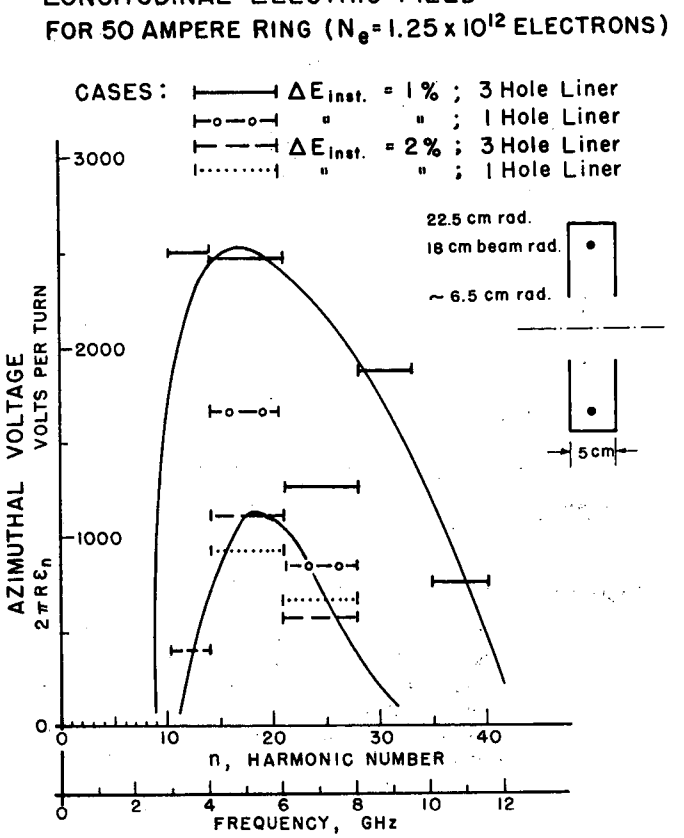

Figure 4 - Plots of maximum radio frequency signal strength for an electron ring current of 50 amperes versus frequency of observation for incident energy spreads of 1% and 2%. The differences between liners having 1 and 3 inflector holes did not appear to be significant.

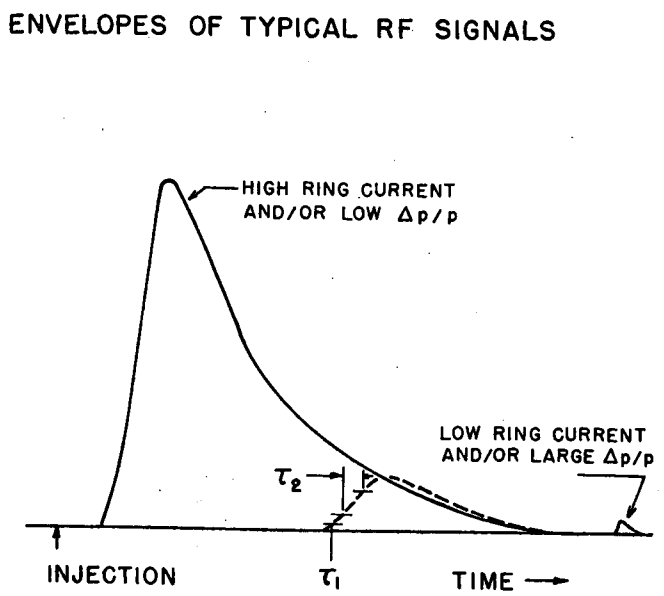

Figure 3 - Sketch of the envelopes of typical R.F. signals. With increasing beam level and/or decreasing incident momentum spread the signals became earlier, stronger, and had faster rates of growth. The shape and timing of the envelopes were the same at all frequency bands where observed.

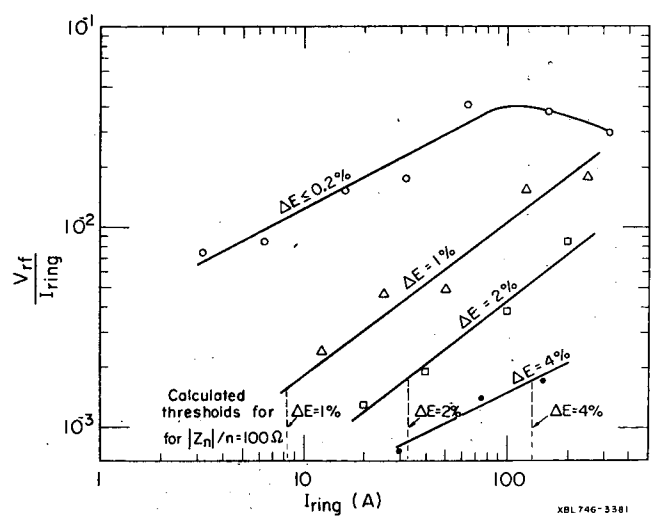

Figure 5 - Plots of relative beam modulation versus trapped ring current for energy spreads of 0.2, 1, 2, and 4%. Observations were in the 2 to 4 GHz frequency band (harmonics 7 to 14) with a two-turn incident beam with energy ramp in a three-hole conducting enclosure.

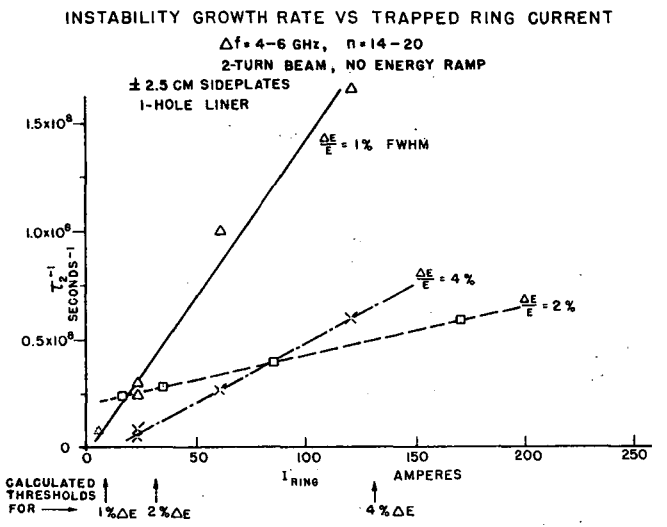

Figure 6 - Plots of growth rate $1/\tau_2$ versus trapped ring current for incident energy spreads of 1 and 2%. Observations in the 4 to 6 GHz frequency band (harmonics 14 to 20) with the two-turn beam without energy ramp in a one-hole enclosure with walls at ± 2.5 cm from the beam mid-plane. The calculated current thresholds for growth of the longitudinal instability assumed $|Zn|/n$ of 100 ohms.

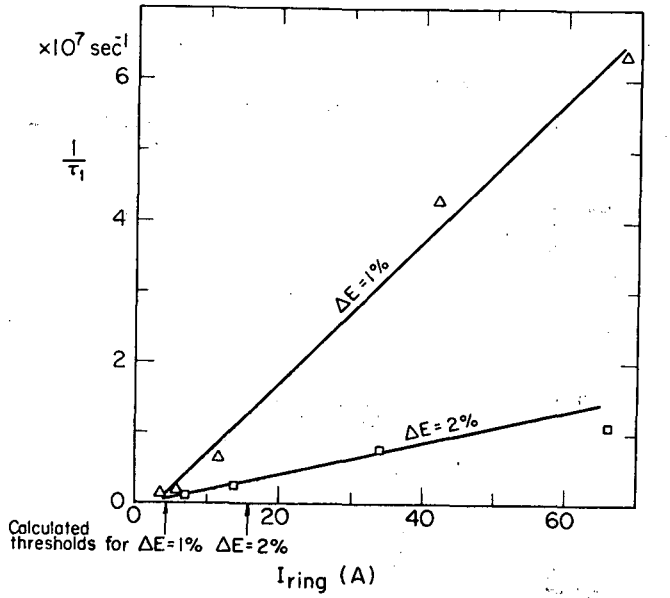

Figure 8 - Plots of growth rate $1/\tau_1$ versus trapped ring current for incident energy spreads of 1 and 2%. Observations in the 4 to 6 GHz frequency band (harmonics 14 to 20) with the half-turn beam in a three-hole enclosure.

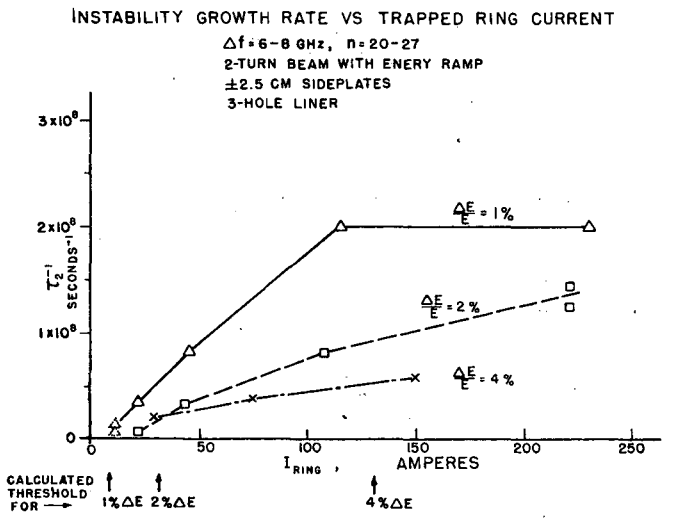

Figure 7 - Plots of growth rate $1/\tau_2$ versus trapped ring current for incident energy spreads of 1 and 2%. Observations in the 6 to 8 GHz frequency band (harmonics 20 to 27) with the two-turn beam with energy ramp in a three-hole enclosure with side-walls at ± 2.5 cm from the beam mid-plane.

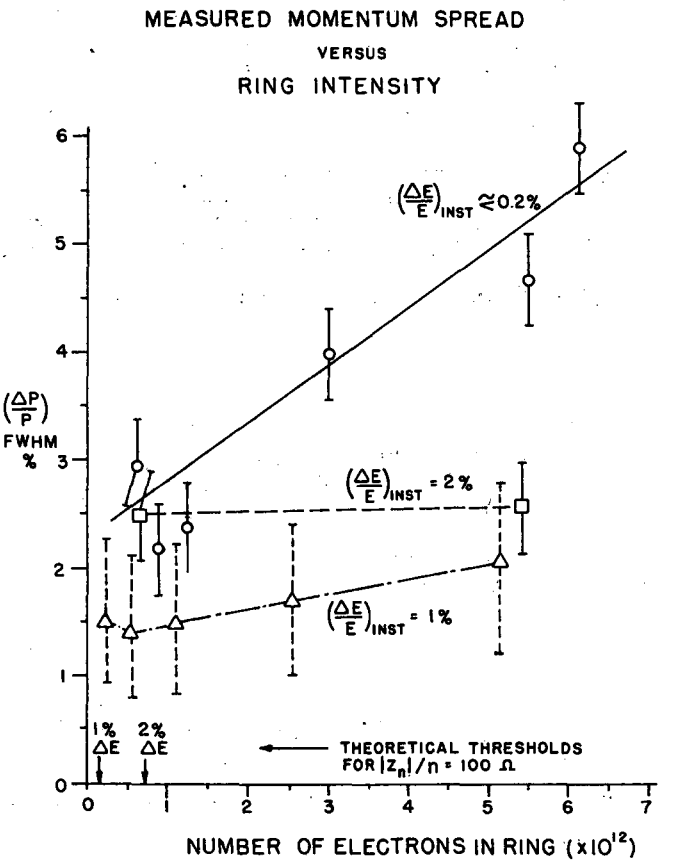

Figure 9 - Plots of the measured final momentum spread versus electron ring intensity for injected instantaneous energy spreads of 0.2, 1, and 2%.

LEGAL NOTICE

This report was prepared as an account of work sponsored by the United States Government. Neither the United States nor the United States Atomic Energy Commission, nor any of their employees, nor any of their contractors, subcontractors, or their employees, makes any warranty, express or implied, or assumes any legal liability or responsibility for the accuracy, completeness or usefulness of any information, apparatus, product or process disclosed, or represents that its use would not infringe privately owned rights.

TECHNICAL INFORMATION DIVISION
LAWRENCE BERKELEY LABORATORY
UNIVERSITY OF CALIFORNIA
BERKELEY, CALIFORNIA 94720